

Water vapor mixing ratios and air temperatures for three martian years from Curiosity

Hannu Savijärvi^{1,2,*}, Timothy H. McConnochie^{3,4}, Ari-Matti Harri², Mark Paton²

¹Institute for Atmospheric and Earth System Research / Physics, University of Helsinki, Finland

²Finnish Meteorological Institute, Helsinki, Finland

³Department of Astronomy, University of Maryland, College Park, MD20742, United States

⁴NASA Goddard Space Flight Center, Greenbelt, MD20771, United States

Revision 1, 11 March 2019

Abstract

The Mars Science Laboratory (MSL) Rover Environmental Monitoring Station humidity instrument (REMS-H) onboard the Curiosity rover is measuring daily minimum water vapor mixing ratios (min vmr), the respective pre-dawn air temperatures (T), and vmr at 2200LT. These are displayed for nearly three martian years (sols 10-2003) and compared with adsorptive column model simulations. The model was initialized with MSL-observed local column water contents, optical depths and surface pressures from sols 230-1291, assuming the same annual cycle outside this period.

The first two and a half MSL years present rather similar annual cycles in the REMS-H data, whereas from about sol 1800 onward the min vmr and T suddenly increase and the 2200LT vmr values get closer to the min vmr, indicating less depletion of water vapor during the nights. Model experiments with typical regolith (ground thermal inertia of 300 SI units and porosity of 30% for adsorption) match the observed min vmr and T relatively well for the first 2.5 years. However, from about sol 1800 onward, when Curiosity started to climb onto Mt. Sharp, simulations with higher thermal inertia of about 400 SI units and very low porosity of ~0.3%, suggesting exposed bedrock, provide a far better fit. Some other periods of bedrock- and dune-dominated ground can be detected from the REMS-H vmr and air-T data along the Curiosity traverse.

Keywords: Mars, climate; Mars, surface; Meteorology

*Corresponding author at: INAR/Physics, Faculty of Science, 00014 University of Helsinki, Finland

E-mail address: hannu.savijarvi@helsinki.fi

Tel: +358-40-9380858

48 1. Introduction

49

50 The Mars Science Laboratory (MSL) onboard the Curiosity rover descended on August 6, 2012
51 onto the Gale crater base (4.6°S, 137.5°E), at L_s 151° of Mars Year (MY) 31. Its Rover
52 Environmental Monitoring Station (REMS, Gomez-Elvira et al., 2012) has among other things
53 made observations of relative humidity (RH) and surface pressure (REMS-H, REMS-P; Harri et al.,
54 2014a, 2014b). The REMS-H instrument measures RH and air temperature T inside a dust-protected
55 but well ventilated cage at 1.6 m height from the surface. The REMS air temperature sensor
56 (REMS-T) and the ground temperature sensor (REMS-GTS) record ambient air and surface
57 temperatures, respectively. The REMS-H and REMS-T measurements of air temperature are quite
58 alike, especially during nighttime when atmospheric turbulence is weak. The REMS-GTS data has
59 been used to chart properties of the ground along the Curiosity track. Hamilton et al. (2014) and
60 Martinez et al. (2014) considered the first 100-150 sols (days), whereas Vasavada et al. (2017) used
61 GTS data from two martian years (1338 sols). These authors have reported variations of ground
62 thermal inertia and albedo along the Curiosity track as derived from the GTS measurements and
63 column modeling, the results being consistent with the orbit retrievals and MastCam pictures of the
64 ground around the rover. In particular, regions of low thermal inertia sand dunes and high thermal
65 inertia exposed bedrock have been detected.

66

67 Here we concentrate on hourly REMS-H measurements of T, RH and the derived water vapor
68 mixing ratio (vmr) of air at 1.6 m height, having data for very nearly three martian years (MSL sols
69 10-2003). Martinez et al. (2017) have discussed the REMS-H daily pre-dawn values of maximum
70 RH and minimum mixing ratio (min vmr) for 1595 sols (more than two martian years), finding that
71 the two annual cycles of daily max RH and min vmr were very similar during this period. The third
72 year now brings a surprise in that after about sol 1800 both T and vmr are much higher during
73 nighttime compared to values during the same season in the previous years. This is analyzed here
74 and the possible reasons are discussed with the help of column modeling. As the near-surface air
75 temperatures tend to stay close to the surface temperatures, it is also studied whether the sol-to-sol
76 variations of the REMS-H air temperatures could be used to chart the apparent thermal inertia of the
77 ground along the Curiosity traverse, thus complementing the GTS findings.

78

79 Our tool is the University of Helsinki/Finnish Meteorological Institute (UH/FMI) column model. Its
80 subsurface scheme for adsorptive regolith was described in Savijärvi et al. (2016), having MSL data
81 from the first 100 sols for validation of the model's diurnal cycle of moisture and temperature. The
82 annual MSL cycle was considered in Savijärvi et al. (2019), forcing the model with the observed
83 REMS-P surface pressures, MastCam optical depths and ChemCam passive mode precipitable
84 water column retrievals (McConnochie et al., 2018) for sols 230-1291. The same annual forcing is
85 applied here, assuming that it remains valid also during the third MSL year. Orbit observations (e.g.
86 the TES and CRISM water columns) have shown little interannual variation in the Gale region apart
87 from periods with large dust events; there were no large dust storms during the third MSL year. The
88 three years of observations and simulations may help to explain and clarify the character of the
89 near-surface moisture and ground properties along the 20 km long Curiosity track from the
90 Bradbury landing site to the slopes of Mt. Sharp by sol 2003.

91

92 The observations and model experiments are described in Section 2. The diurnal cycles of REMS-H
93 T, RH and vmr are displayed around L_s 90° in Section 3 before and after sol 1800, together with
94 some illustrative model simulations for varied ground properties. The three-year daily observations
95 and simulations are then considered and discussed in Sections 4 and 5. Conclusions are drawn in
96 Section 6.

97

98

99

100 2. Observations and model experiments

101

102 We use here the hourly REMS-H observations of T and RH, and the derived water vapor volume
 103 mixing ratio $\text{vmr} = \text{RH}e_{\text{sat}}(T)/p$, where $e_{\text{sat}}(T)$ is the saturation water vapor pressure over ice, and p
 104 is the surface pressure measured by the REMS-P instrument (Harri et al., 2014a; 2014b). The hourly
 105 data (T, RH and vmr at 1.6 m height) is from sols 10-2003 (nearly three martian years of 669 sols),
 106 but we concentrate here mainly on the daily minimum values of vmr (min vmr) and the respective T
 107 at the time of min vmr (~max RH), typically during the early morning. The daytime maxima of vmr
 108 are also considered but since the measured daytime RH is very small and inaccurate due to
 109 instrument limitations, the daytime and early evening values for the vmr are unreliable. Hence the
 110 vmr at 2200LT is taken as a proxy for maximum vmr. Error bars for the nighttime RH are about +/-
 111 10%. Some full diurnal cycles of the measured REMS-H T, RH and vmr are displayed in Figure 2
 112 for 2-3 sols. The variability between the hourly observations is a measure of the typical sol-to-sol
 113 variance.

114

115 Use is also made of local column precipitable water content retrievals (PWC) from the ChemCam
 116 passive mode spectral sky scans, 880 nm total column optical depths (τ , mostly dust) from the
 117 MastCam, and p from REMS-P for sols 230-1293, as described in McConnochie et al. (2018). It
 118 was shown in Savijärvi et al. (2019) that the well mixed vmr based on the daytime ChemCam PWC
 119 is close to the midday MSL site surface vmr in the GCM-based Mars Climate Database (MCD)
 120 during all seasons. Hence the ChemCam vmr can be used as a local estimate for the daytime near-
 121 surface vmr along the Curiosity traverse.

122

123 The UH/FMI atmosphere-subsurface model and its application is here the same as in Savijärvi et al.
 124 (2019). It is a hydrostatic single column model driven by a constant geostrophic wind in assumedly
 125 horizontally homogeneous conditions (hence there are no advection terms). Wind shear- and
 126 convective-driven turbulence, radiation and cloud physics drive the evolution of wind, temperature,
 127 moisture and clouds/fogs in the atmospheric column (28 gridpoints from 0.3 m to 50 km). Thermal
 128 diffusion for temperature and molecular/Knudsen diffusion with possible adsorption of moisture
 129 onto regolith grains via the Jakosky et al. (1997) adsorption isotherm (J97) govern the evolution of
 130 soil temperature and pore volume moisture in eight gridpoints from 0 to 50 cm depth. The Zent and
 131 Quinn (1997, Z97) and Fanale and Cannon (1971, F71) adsorption isotherms were also tried, but
 132 the Z97 isotherm produces in our framework practically the same results as J97, whereas F71
 133 exhibits excessive daytime desorption, as it did in Savijärvi et al. (2016) and Steele et al. (2017).

134

135 The radiation scheme was compared with the reference line-by-line model results in Savijärvi et al.
 136 (2005) for CO₂, H₂O and dust, leading to a fairly accurate improved delta-discrete-ordinate method
 137 (iDD) for shortwave multiple scattering in a dusty atmosphere. Values for the dust broadband single
 138 scattering albedo (0.90), asymmetry parameter (0.70), and $\tau_{\text{vis}}/\tau_{\text{IR}}$ ratio (2.0) were checked by Mie
 139 calculations for Wolff et al. (2009) dust optics in Savijärvi (2012), where also the physics of the
 140 typical diurnal cycle in the boundary layer of Mars was discussed in detail, using the Spirit mini-
 141 TES observations (Smith et al., 2006) for validation. The model results have also been compared
 142 with the observations from Pathfinder (Savijärvi et al., 2004), Phoenix (Savijärvi and Määttänen,
 143 2010) and the Viking landers (Savijärvi et al., 2018).

144

145 In the present Curiosity simulations the latitude is 4.6°S and L_s defines the season. Surface
 146 roughness length is 0.01 m, albedo 0.20 and infrared emissivity 0.96. Soil thermal inertia I and
 147 porosity may vary. The model is initialized from MSL-observed values for vmr, τ and p and is run
 148 to model sol 3, by which time it has spun up to a repeating diurnal cycle of temperatures, winds and
 149 moistures. Soil porosity is 30% and thermal inertia I is 300 J m⁻² K⁻¹ s^{-1/2} (SI units, omitted
 150 hereafter), unless stated otherwise. Geostrophic wind is 10 ms⁻¹, leading to surface winds of about 5
 151 ms⁻¹ during daytime and 3 ms⁻¹ during the nights. The results shown are from the model sol 3.

152
153
154
155
156
157
158
159
160
161
162
163
164
165
166
167
168
169
170
171
172
173
174
175
176
177
178
179
180
181
182
183
184
185
186
187
188
189
190
191
192
193
194
195
196
197
198
199
200
201
202
203

The seasonal water ice cloud parameterization of Vasavada et al. (2017) is not used, because ice clouds are already included in the total observed optical depth τ , and the model results do not indicate any notable systematic seasonal deviations from the observations.

3. Results: REMS-H diurnal cycles around $L_s 90^\circ$ at MY32 and MY34

All the available three martian year REMS-H observations (sols 10-2003) for each diurnal hourly minima and maxima of the volume mixing ratio are shown in Figure 1. The daily minima (min vmr) typically occur at about 0400-0600 local solar time (LT), when the observed relative humidity reaches its diurnal maximum (cf. Figure 2). The maxima of vmr (max vmr) are from 2200LT, as the daytime vmr values are unreliable due to the then very low relative humidity.

Figure 1 displays a repeating annual pattern, where the minima of both max and min vmr are obtained during the cool aphelion – southern late fall seasons at Gale, ie. around $L_s 90^\circ$ (dashed upright lines), and the annual maxima respectively during the warm seasons around $L_s 270^\circ$ (solid upright lines). The 2200LT vmr (max vmr) are always higher than the minima of vmr from the next morning. This indicates a depletion process during every night, probably by adsorption of water vapor into cold regolith grains, followed by desorption back to vapor phase after sunrise.

A striking exception to this annual pattern in Figure 1 is, however, the rapid rise in the vmr values after about sol 1800. Thereafter also the max and min of vmr tend to stay closer together, indicating less depletion during the night. For a closer look we next display the full diurnal cycles of T, RH and vmr at around $L_s 90^\circ$ before and after sol 1800. The measured nocturnal relative humidities are high and most accurate during this season; hence the values of the derived vmr are also at their most accurate, although they are small. The values of min vmr around $L_s 90^\circ$ are about 15-17 ppmv both at MY32 and at MY33 in Figure 1, whereas those after sol 1800 (at MY34) are much higher, around 50 ppmv; or threefold.

Figure 2 displays all the available REMS-H hourly observations of T, RH and vmr for sols 541-543 ($L_s 90^\circ$ MY32) as white marks, and for sols 1880-1881 ($L_s 90^\circ$ MY34) as black marks. One may note that during the night T is consistently about 5 K higher at MY34 than at MY32, and RH is also slightly higher, whereas vmr is considerably higher at MY34 than at MY32. The hourly sol-to-sol variation is notable in RH but small in the observations of T and vmr.

In order to try and explain the big $L_s 90^\circ$ differences between MY32 and MY34, column model experiments are made. In Savijärvi et al. (2019) the UH/FMI atmosphere-regolith model was initialized by the sol 543 MSL observations: ChemCam PWC 5.31 μm , τ 0.41, p 8.44 mb. This $L_s 90^\circ$ MY32 simulation with I 300 and porosity 30% as for typical regolith is shown in Figure 2 via solid lines. Its results match the sol 541-543 REMS-H T observations quite well (except for the turbulent early afternoon); they underestimate the nocturnal RH observations to some extent, but are quite close to the observed MY32 nocturnal vmr, matching the observed pre-dawn minimum vmr of about 15 ppmv. The model's midday vmr is on the other hand close to the ChemCam 11:43LT vmr of 56 ppmv (X in Figure 2). The depletion of the model's vmr from 1600LT onward in Figure 2 is due to downward diffusion and adsorption into the rapidly cooling soil; the increase after sunrise is due to desorption and upward diffusion from the sun-heated regolith. The regolith simulation (solid lines) matches the white MY32 vmr observations quite well during nighttime. In contrast, it does not fit at all the black MY34 observations of T and vmr.

Because the high observed nighttime temperatures and mixing ratios during sols 1880-1881 may hint at a more rocky ground with higher thermal inertia and hence smaller amplitude of the diurnal

204 surface and near-surface air temperature cycle, model experiments were repeated by increasing I
 205 and/or decreasing porosity. The forcing (PWC, τ , p) was kept the same as for MY32, because the
 206 first two years appeared rather similar by Figure 1, and the ChemCam PWC retrievals for MY34
 207 were not yet available. A good match with the sol 1880-1881 REMS-H observations was obtained
 208 by increasing I to 400 and setting porosity to only 0.3%, or 0.1%. These two ‘rock’ experiments are
 209 shown in Figure 2 by the dotted and dashed lines. They fit the black MY34 observations fairly well,
 210 displaying both the systematic increase of 5 K in nocturnal T and the high pre-dawn vmr values of
 211 about 50 ppmv. On the other hand, the simulation with high I and high porosity (30%; dash-dot
 212 lines) produces the high nocturnal T (all three ‘rock’ I=400 experiments displaying identical T-
 213 curves in Figure 2), but not the high nocturnal RH and vmr, because of the now active evening
 214 depletion of water vapor by adsorption.

215

216 Reduced ground porosity hence appears essential to the increased nocturnal vmr for sols 1880-
 217 1881, nearly independently of thermal inertia, whereas increased thermal inertia is responsible for
 218 the increase in the nocturnal temperatures, independently of ground porosity.

219

220 Hence we suggest that 1) the annual environmental conditions at Gale remained presumably rather
 221 similar during the three martian years. For the two first years this was the case according to
 222 Martinez al. (2017) and Vasavada et al. (2017). However, the rover encountered quite variable
 223 ground along its travel. As an example, Figure 3 demonstrates a MastCam view from sol 1812,
 224 when the rover has begun climbing up (from about sol 1800 onward) the Vera Rubin ridge at the
 225 foot of Mt. Sharp. The dark landing plane on the left is largely covered by dusty loose material
 226 (regolith) with low thermal inertia and high porosity, whereas the ridge in front of the rover is
 227 mainly higher inertia nonadsorptive solid exposed bedrock with just a hint of wind-blown
 228 adsorptive shallow dust here and there. It is therefore suggested that 2) the observed increases in
 229 REMS-H min vmr and T at 1.6 m after about sol 1800 are mainly due to the exposed bedrock
 230 encountered by the rover at the foot of Mt. Sharp.

231

232 The thermophysical properties of the ground along the rover’s traverse at Gale were analyzed in
 233 detail from the REMS GTS data for the first two MSL years in Vasavada et al. (2017). In the next
 234 sections we use the three-year REMS-H vmr and T data for the same purpose in a simplified but
 235 perhaps illuminating fashion. For this it is noteworthy in Figure 2 that the model’s L_s 90° night
 236 temperatures match the observed temperatures almost perfectly with a suitable thermal inertia. The
 237 estimation of thermal inertia is considered in Section 4. Furthermore, as the water vapor mixing
 238 ratios are very sensitive to temperature (because of the steep $e_{\text{sat}}(T)$ relation), it is then essential for
 239 realistic vmr results and hence realistic ground porosity estimates (Section 5) that the model’s
 240 temperatures are accurate.

241

242

243 **4. Annual experiments: REMS-H temperatures and ground thermal inertia**

244

245 Annual results are here discussed for the daily 1.6 m REMS-H temperatures at the time of min vmr,
 246 and compared with the respective pre-dawn T at 1.6 m height from the model simulations. The
 247 model is initialized at L_s 45° steps from approximate fits (connected by lines in Figure 4) to the
 248 MSL-observed PWC, τ and p from sols 230-1293 from McConnochie et al. (2018). The same
 249 annual forcing of PWC, τ and p is then used outside this range, hence assuming an unchanging
 250 annual environment at Gale. As a result, the annual model curves repeat themselves; this can be
 251 used for reference purposes. The model’s ground surface temperatures for I = 300 produce similar
 252 daily ranges to the GTS-observed T_g in Vasavada et al. (2017) and Martinez et al. (2017), ie. about
 253 205-290K during the warm season and 185-255K during the cold season.

254

255 Figure 5 displays the REMS-H -observed T of min vmr together with the respective model-T. The

256 three model lines correspond to ground thermal inertias I of 250, 300 and 400. The $I = 300$ curve
 257 (solid line) appears to give a decent overall fit for sols 10-1800 even outside the data-based MY32
 258 forcing period (bold solid). This suggests that the annual forcing remained much the same.
 259 However, from about sol 1800 onward, the $I = 400$ curve gives a much better overall match, as it
 260 did in Figure 2. Generally the T observations remain within the I 250-400 model lines.

261
 262 An interesting feature appears in the dotted range of sols 55-100 in Figure 5 (L_s 180°-210°, MY31),
 263 when Curiosity was parked on a loose-material sand dune region “Rocknest”. Here the observed
 264 REMS- T values tend to fall below the $I = 300$ model curve. Martinez et al. (2014) and Vasavada et
 265 al. (2017) derived I of 295 and 250-300 for this site, respectively. Curiosity then traversed on rocky
 266 ground during sols 120-350 (L_s 225°-360°, MY31). Martinez et al. obtained I of 452 for sol 139,
 267 while Vasavada et al. indicate I of 350-450 for this high- I period. Figure 5 suggests that the REMS-
 268 H T -values stay mainly between the T -lines from the $I = 300$ and $I = 400$ simulations during this
 269 period, while some high observed values of the pre-dawn T hint to I occasionally perhaps exceeding
 270 400 SI units.

271
 272 Other high- I periods in Vasavada et al. are sols 800-900, and especially sols 1100-1170 and 1250-
 273 1350. These periods correspond to the observed REMS-H T being well above the T from the $I =$
 274 300 simulation in Figure 5. Respectively, the low- I periods in Vasavada et al. during sols 500-540,
 275 and especially sols 1222-1242 (Namib Dune), are associated with the observed T being below the T
 276 from the $I = 300$ simulation in Figure 5. Hence the REMS-H air- T -observations appear to provide
 277 potential for the estimation of thermal inertia along the Curiosity track, thereby confirming and
 278 complementing the more direct GTS-based estimates.

279
 280

281 **5. Annual experiments: REMS-H water vapor mixing ratios and ground porosity**

282
 283 Figure 6 displays all the available REMS-H daily minima of vmr (min vmr) for three martian years;
 284 the respective air temperatures were shown in Figure 5. Shown are also the lines for the daily
 285 minima of vmr at 1.6 m height from two model simulations. The reference simulation (I 300,
 286 porosity 0.30, solid line) is forced by the ChemCam–based local PWC at L_s 45° steps (Figure 4).
 287 This simulation is quite good during the first two cool seasons with low min vmr . During the warm
 288 seasons with higher, less accurate and more variable min vmr it tends, however, to produce lower
 289 values than those observed. During the warm seasons the other simulation (dashed line) appears to
 290 provide a better fit. There the initial PWC is made 3 μm higher than the local ChemCam retrieval,
 291 and hence closer to the large-scale TES and CRISM retrievals for the Gale region from the orbit
 292 (McConnochie et al., 2018; Savijärvi et al., 2019). Perhaps the “flushing” large-scale winds of the
 293 warm season (Rafkin et al., 2016) are able to mix the higher moisture content of the surrounding
 294 areas into the crater. The crater appears more isolated and dominated by local circulations during
 295 the other seasons.

296
 297 The Rocknest stay stands out in Figure 6 as a low min vmr period within the moist season of high
 298 observed PWC and high model min vmr . In comparison to the other two respective seasons, Figure
 299 6 implies that the small observed min vmr during the Rocknest stay is exceptional, indicating strong
 300 adsorption during the nights, and hence presumably high porosity of the ground. Low T and low
 301 thermal inertia were also characteristic for the Rocknest period in Figure 5. Hence the ground is
 302 likely that of finely-grained sand dune -like adsorptive regolith. The MastCam pictures of Martinez
 303 et al. (2014) confirm this. The Namib Dune period (sols 1222-1242) is also associated with low T
 304 and low min vmr in Figures 5 and 6. Thus the excessively high values of T and min vmr beyond sol
 305 1800 may indicate the opposite, ie. exposed nonadsorptive bedrock; but other possible explanations
 306 should first be ruled out.

307

308 Remarkably, the increased but still realistic moisture input (dashed line) is not able to increase the
 309 model's min vmr enough in Figure 6 to match the high observed min vmr after sol 1800. The good
 310 match of the reference simulation before sol 1800 suggests no big changes in the large-scale
 311 circulation. The observed MastCam optical depths likewise support the repeating annual
 312 environmental conditions; for instance the increase in τ due to the MY34 dust storm is observed at
 313 Gale only beyond sol 2070. The reason for the high vmr values must hence lie elsewhere. At sol
 314 1880 (Figure 2) the rover is located about 10 km to south-west (toward Mt. Sharp) from the landing
 315 site, and has climbed about 350 m on the way. Could this change in position and altitude explain the
 316 observed increases in the pre-dawn T and min vmr? In contrast, the Gale cool season mesoscale
 317 simulations of Steele et al. (2017; figs. 26d, 28c, 30e) suggest that at 0600LT the near-surface pre-
 318 dawn air temperatures *decrease* from the landing site toward Mt. Sharp, because downslope
 319 katabatic winds have piled adiabatically heated warmer air to the crater base during the night. (This
 320 warming effect has been described for Mars in Spiga et al. (2009) and Rafkin et al. (2016), and for
 321 Antarctic slopes in Savijärvi (2011)). The 0600LT near-surface mixing ratios do increase slowly
 322 uphill in the Steele et al. simulation, but only very modestly along the 10 km distance from the MSL
 323 landing site to the sol 1880 site.

324
 325 Hence the explanation lies probably in the ground properties along the track. Figure 7 displays all
 326 the observed REMS-H daily maximum and minimum values of vmr with the min vmr from two
 327 annual simulations: the reference "regolith" case with I 300 and porosity 0.30 (solid line), and the
 328 "exposed bedrock" case with I 400 and porosity 0.003 (dashed line). The regolith simulation gives a
 329 decent fit to the observed min vmr until about sol 1500, after which it fails more or less. The rock
 330 simulation is on the other hand clearly not very good for the first 2.5 years, but from about sol 1800
 331 onward it begins to match the min vmr observations very well in Figure 7. The rock simulation (I
 332 400) also matches the observed pre-dawn temperatures beyond sol 1800 (Figures 2 and 5).
 333 Furthermore, from sol 1800 onward the observed maxima and minima of vmr tend to stay closer
 334 together than they did before, indicating less nocturnal adsorption. Hence we suggest that the
 335 exposed bedrock at the foot of Mt. Sharp is the main explanation for the change in the behavior of
 336 the REMS-H T and vmr after about sol 1800 along the Curiosity traverse.

337
 338 The maxima of vmr since sol 1800 are somewhat higher than during the previous cold seasons.
 339 Increased moisture contents above Gale could perhaps explain some of the increase. However, in
 340 Figure 6 the simulation with increased PWC was not able to increase the vmr enough. Furthermore,
 341 most of the adsorption presumably takes place during the late afternoon and early evening, as in
 342 Figure 2 (and as observed at Phoenix, Zent et al., 2016). Hence, during weak or no adsorption, as
 343 over exposed bedrock, the vmr at 2200LT is already quite close to the min vmr of the next morning.
 344

345 Finally, the Rocknest and Namib dune periods stand out in Figures 1 and 7 in that the relative
 346 difference between the observed max and min vmr is enhanced compared to the surrounding sols,
 347 indicating more depletion during the night. These sites, which are dominated by loose material
 348 regolith, thus appear opposite in their behavior of vmr to the solid bedrock -dominated climb from
 349 sol 1800 onward.

352 6. Conclusions

353
 354 The daily 2200LT water vapor mixing ratios (max vmr), the pre-dawn minimum values (min vmr)
 355 and the air temperatures (T) of min vmr from the MSL REMS-H instrument were shown for three
 356 martian years, and compared with predictions from a subsurface-atmosphere column model with
 357 adsorption to regolith grains. The model was forced at 45° L_s steps by mean local column
 358 precipitable water contents, optical depths and air pressures based on MSL measurements from sols
 359 230-1291, assuming the same (mainly MY32) annual cycle outside the measurement period.

360
361
362
363
364
365
366
367
368
369
370
371
372
373
374
375
376
377
378
379
380
381
382
383
384
385
386
387
388
389
390
391
392
393
394
395
396
397
398
399
400
401
402
403
404
405
406
407
408
409
410
411
412
413

The first two and a half MSL years indicate rather similar annual cycles in the observed 2200LT vmr, min vmr and T. These display low values during the cool seasons and high values during the warm seasons. From about sol 1800 onward they suddenly increase, T being about 5K above its previous values from the same season, and min vmr increasing by a factor of 3. Furthermore, the 2200LT evening values of vmr, which are always greater than the min vmr, then get closer to min vmr, indicating less depletion of near-surface air water vapor during the nights. Model experiments with ground thermal inertia of 300 SI units and porosity of 30% for adsorption, as for typical regolith, fit the observed REMS-H min vmr and T relatively well in general for the first two and a half years, but not thereafter.

Instead, from about sol 1800 onward, when Curiosity started to climb onto Mt. Sharp, the simulations with a higher I of about 400 SI units and very low porosity of ~0.3% (both as for exposed bedrock) produce a better fit. MastCam pictures from this time verify the expected bedrock scenery with very sparse and thin layers of wind-blown dust. Some other bedrock- and dune - dominated periods can be detected from the REMS-H data. These periods agree with the previous more direct REMS-GTS -based estimates of the ground type encountered along the Curiosity traverse.

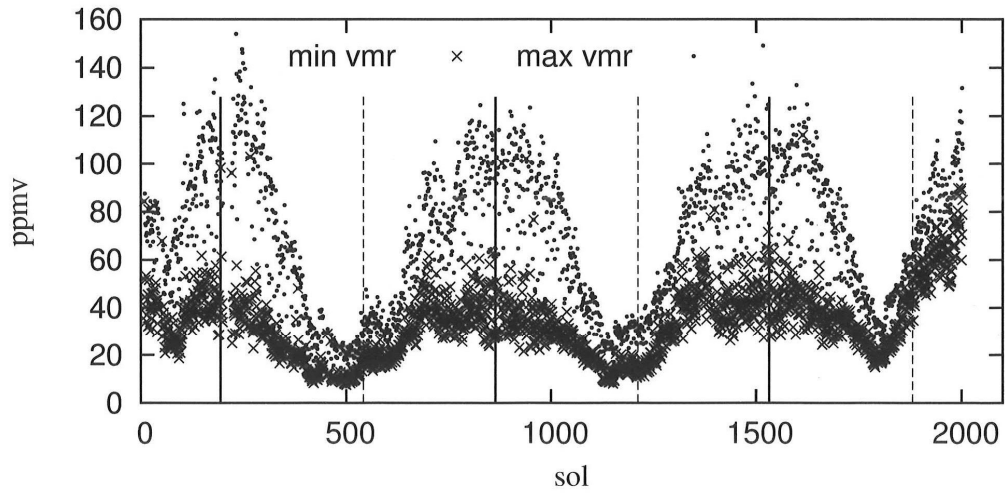
Acknowledgements: The work was supported by the Academy of Finland grants 131723, 132825 and 310509. We thank the reviewers for thoughtful comments that helped to improve the article.

References:

- Fanale FP, Cannon WA, 1971: Adsorption on the martian regolith. *Nature* 230, 502-504.
- Gómez-Elvira GJ et al., 2012. REMS: The Environmental Sensor Suite for the Mars Science Laboratory Rover. *Space Sci. Rev.* 170, 583-640, doi:10.1007/s11214-012-9921-1.
- Hamilton VE et al., 2014. Observations and preliminary science results from the first 100 sols of MSL REMS ground temperature sensor measurements at Gale crater. *J.Geophys.Res.* 119, 745-770. doi:10.1002/2013JE004520.
- Harri AM, et al., 2014a. Mars Science Laboratory relative humidity observations: initial results. *J. Geoph. Res. Planets* 119, 2132-2147, doi: 10.1002/2013JE004514
- Harri AM, et al., 2014b. Pressure observations by the Curiosity rover: initial results. *J.Geophys.Res. Planets* 119, 82-92. doi: 10.1002/2013JE004423.
- Jakosky BM, Zent AP, Zurek RW, 1997. The Mars water cycle: Determining the role of exchange with the regolith. *Icarus* 130, 87-95.
- Martinez GM et al., 2014. Surface energy budget and thermal inertia at Gale crater: calculations from ground-based measurements. *J.Geophys.Res.* 119, 1822-1838.
- Martínez GM, Newman CN, De Vicente-Retortillo A, Fischer E, Renno NO, Richardson MI, Fairén AG, Genzer M, Guzewich SD, Haberle RM, Harri AM, 2017. The Modern Near-Surface Martian Climate: A Review of In-situ Meteorological Data from Viking to Curiosity. *Space Sci. Rev.* pp.1-44.
- McConnochie TH, et al., 2018. Retrieval of water vapor column abundance and aerosol properties from ChemCam passive sky spectroscopy. *Icarus* 307, 294-326, doi:10.1016/j.icarus.2017.10.043.

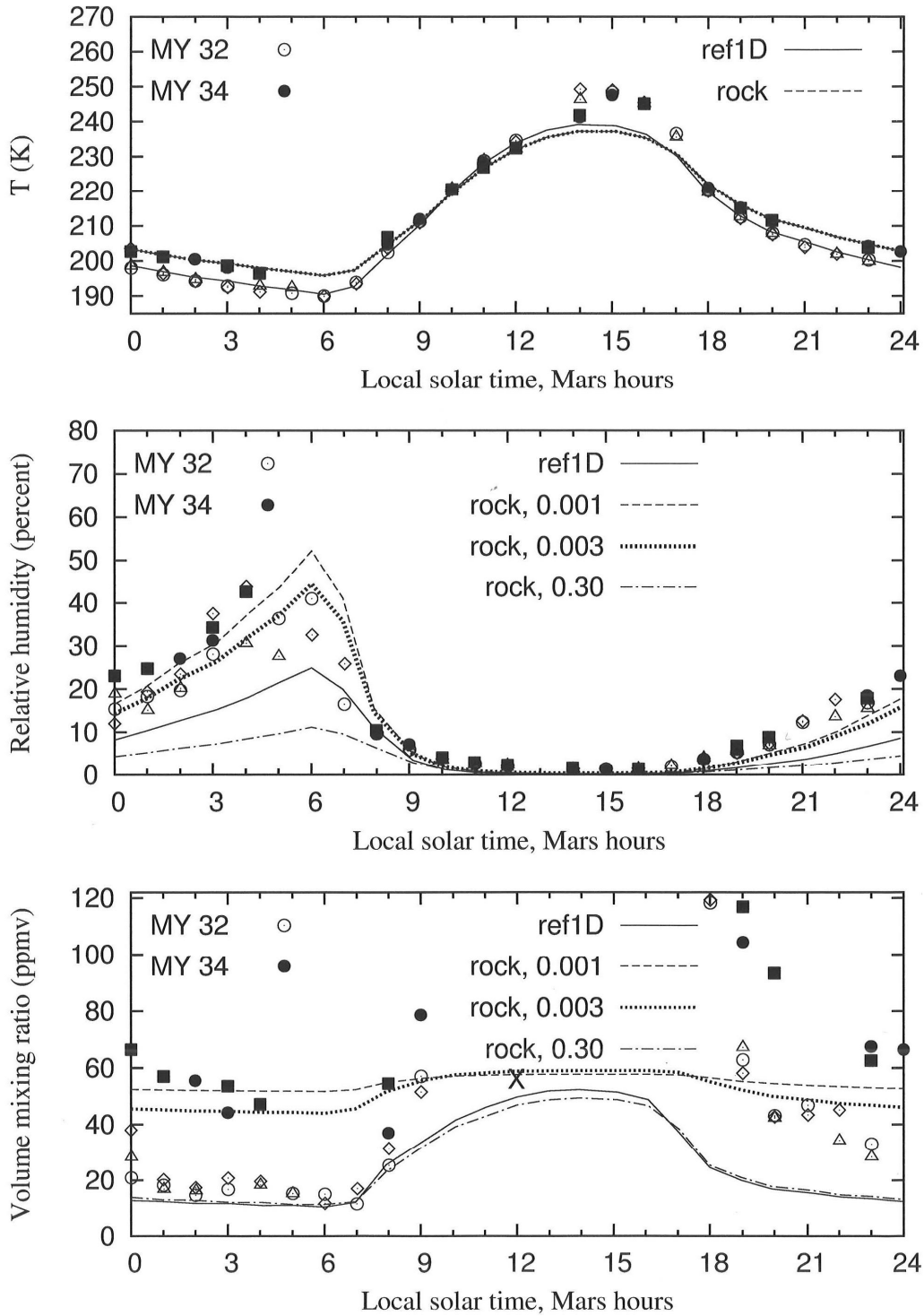
- 414 Rafkin S et al., 2016. The meteorology of Gale Crater as determined from Rover Environmental Monitoring
415 Station observations and numerical modeling. Part II: Interpretation. *Icarus*, doi:10.1016/j.icarus.2016.01.03.
416
- 417 Savijärvi, H., A. Määttänen, J. Kauhanen and A-M. Harri, 2004: Mars Pathfinder: new data and new model
418 simulations. *Quart.J.Roy.Meteor.Soc.*, 130, 669-683.
419
- 420 Savijärvi, H., D. Crisp, and A.-M. Harri, 2005: Effects of CO₂ and dust on present-day solar radiation and
421 climate in Mars. *Quart.J.Roy.Meteor.Soc.*, 131, 2907-2922.
422
- 423 Savijärvi, H, A. Määttänen, 2010: Boundary-layer simulations for the Mars Phoenix lander site. *Quart. J.*
424 *Roy. Meteor. Soc.*, 136, 1497-1505, doi:10.1002/qj.650
425
- 426 Savijärvi, H, 2011: Antarctic local wind dynamics and polynya effects on the Adelie Land coast. *Quart. J.*
427 *Roy. Meteor. Soc.* 137, 1804-1811. doi:10.1002/qj.874
428
- 429 Savijärvi, H., 2012: Mechanisms of the diurnal cycle in the atmospheric boundary layer of Mars. *Quart. J.*
430 *Roy. Meteor. Soc.* 138, 552-560. doi:10.1002/qj.930
431
- 432 Savijärvi H, A-M Harri, O Kempainen, 2016: The diurnal water cycle at Curiosity: role of exchange with
433 the regolith. *Icarus* 265, 63-69, doi:10.1016/j.icarus.2015.10.008
434
- 435 Savijärvi H, M Paton, A-M Harri, 2018: New column simulations for the Viking landers: winds, fog, frost,
436 adsorption? *Icarus* 310, 48-53, doi: 10.1016/j.icarus.2017.11.007
437
- 438 Savijärvi H, T McConnochie, A-M Harri, M Paton, 2019: Annual and diurnal water vapor cycles at Curiosity
439 from observations and column modeling. *Icarus* 319, 485-490. doi:10.1016/j.icarus.2018.10.008
440
- 441 Smith MD, Wolff MJ, Spanovich N, Ghosh A, Banfield D, Christensen PR, Landing GA, Squyres SW, 2006.
442 One Martian year of atmospheric observations using MER Mini-TES. *J.Geophys.Res. Planets* 111, E12513.
443
- 444 Spiga A, Forget F, 2009. A new model to simulate the Martian mesoscale and microscale atmospheric
445 circulation: Validation and first results. *J.Geophys.Res.* 114 E2. doi:10.1029/2008JE003242
446
- 447 Steele LJ, Balme MR, Lewis SR, Spiga A, 2017. The water cycle and regolith-atmosphere interaction at Gale
448 crater, Mars. *Icarus* 280, 56-79.
449
- 450 Vasavada AR, Piqueux S, Lewis KW, Lemmon MT, Smith MD, 2017. Thermophysical properties along
451 Curiosity's traverse in Gale crater, Mars, derived from the REMS ground temperature sensor. *Icarus* 284,
452 372-386. doi:10.1016/j.icarus.2016.11.035.
453
- 454 Wolff, M. J., M. D Smith, R.T. Clancy, R. Arvidson, M. Kahre, F. Seelos IV, S. Murchie, and H. Savijärvi,
455 2009: Wavelength dependence of dust aerosol single scattering albedo as observed by the Compact
456 Reconnaissance Imaging Spectrometer. *J.Geophys.Res.*, 114, E00D04, doi:10.1029/2009JE003350.
457
- 458 Zent AP, Hecht MH, Hudson TL, Wood SE, Chevrier VF, 2016. A revised calibration function and results for
459 the Phoenix mission TECP relative humidity sensor. *J. Geophys. Res. (Planets)* 121, 626-651.
460
- 461 Zent AP, Quinn RC, 1997: Measurement of H₂O adsorption under Mars-like conditions: Effects of adsorbent
462 heterogeneity. *J.Geophys.Res.* 102 (E4), 9085-9095.
463

465 **Figures:**
 466
 467
 468



469
 470
 471
 472
 473
 474
 475

Figure 1. The daily pre-dawn minimum water vapor volume mixing ratios (min vmr; dark crosses) and the 2200LT mixing ratios (max vmr; dots) from REMS-H for MSL sols 10-2003. Solid upright lines indicate $L_s 270^\circ$ (warm season at Gale), dashed upright lines indicate $L_s 90^\circ$ (cool season at Gale). Temperatures at the hour of min vmr are shown in Figure 5.

476
477478
479

480

481

482

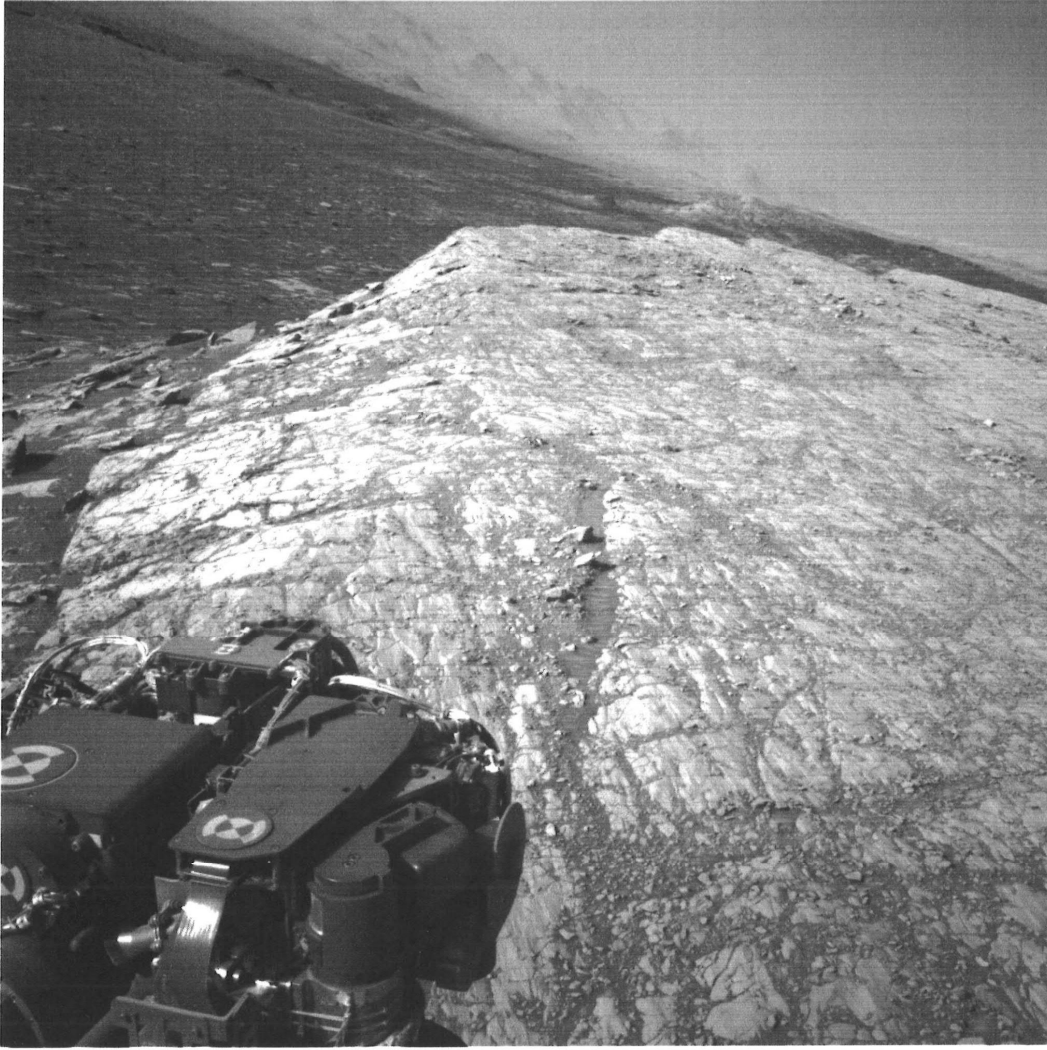
483

484

485

Figure 2. The hourly T, RH and vmr at 1.6 m around $L_s 90^\circ$ from REMS-H (MY 32 in white; MY 34 in black), and from column model simulations: “ref1D”: $I = 300$, porosity 0.30, solid lines; “rock”: $I = 400$ with porosity 0.001 dashed; 0.003 dotted; 0.30 dash-dotted. Open diamonds, spheres and triangles are from sols 541, 542, 543, respectively; filled spheres and squares from sols 1880, 1881, respectively. X is the ChemCam 11:45 LT vmr observation from sol 543.

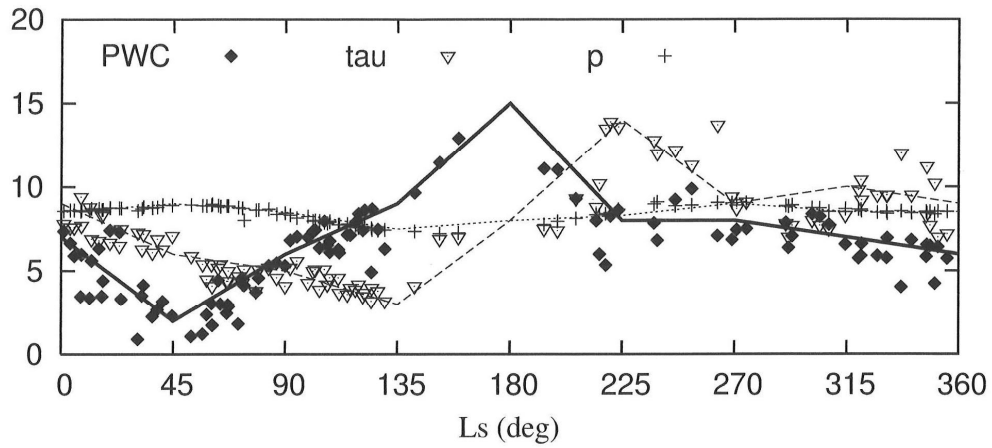
486



487
488
489
490

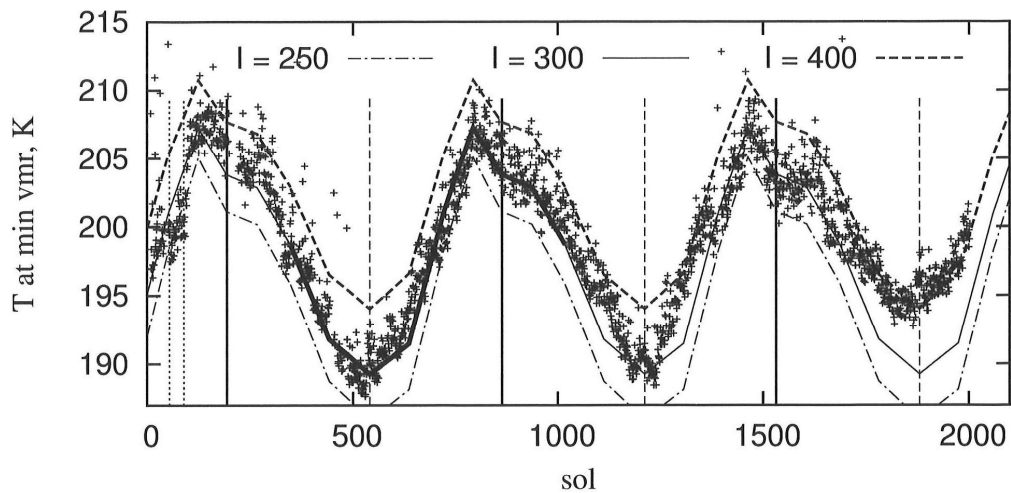
Figure 3. MastCam picture from Curiosity climbing up the rocky Vera Rubin Ridge at the base of Mt. Sharp on sol 1812. On the left the regolith-dominated crater base where the landing took place.

491



492
493
494
495
496
497
498
499
500
501

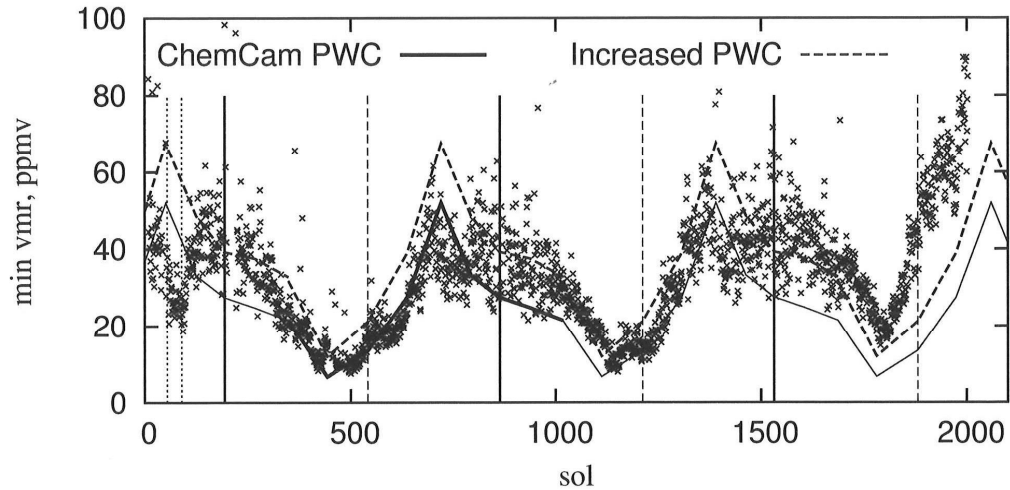
Figure 4. Column precipitable water content (PWC, in μm) from ChemCam passive sky scans, column total opacity, mostly by dust (τ multiplied by 10) from MastCam, and surface pressure (p, in mb) from REMS-P (McConnochie et al., 2018), and approximate fits to these data at L_s 45° steps (lines) for the model's annual forcing.



502
503
504
505
506
507
508
509
510
511
512
513
514
515

Figure 5. The daily 1.6 m REMS-H air temperatures at the pre-dawn hour of min vmr for MSL sols 10-2003, and column model 1.6 m min vmr temperatures for ground thermal inertias of 250, 300 and 400 SI units. The data-based model forcing period (MY32) is in bold in the I 300 curve. Solid upright lines indicate L_s 270° (warm season at Gale), dashed upright lines indicate L_s 90° (cool season at Gale). The Rocknest dune stay (sols 55-100) is marked by the dotted upright lines.

516



517

518

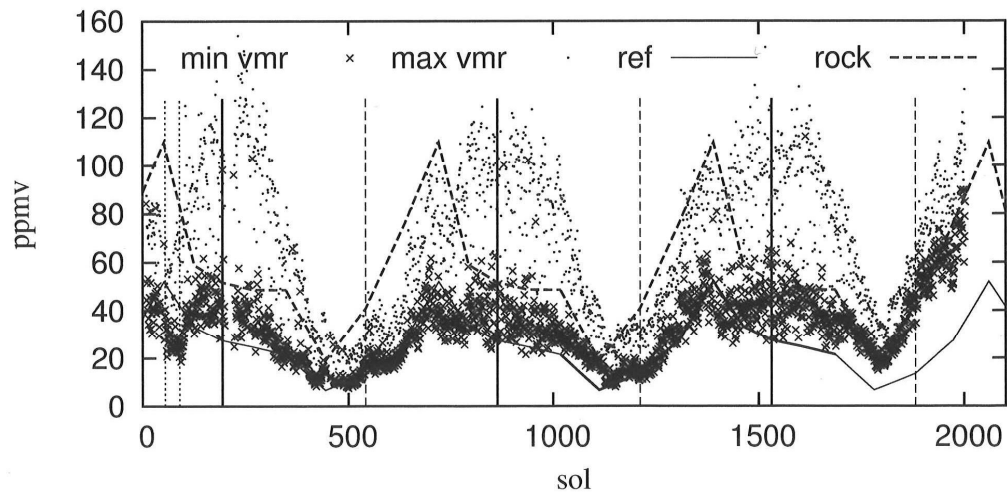
519 Figure 6. The daily REMS-H min vmr for MSL sols 10-2003, and the min vmr from the model (I
 520 300, porosity 0.30) forced by ChemCam PWC, and by ChemCam PWC + 3 μm . The Rocknest dune
 521 stay (sols 55-100) is marked by the dotted upright lines.

522

523

524

525



526

527

528 Figure 7. The daily min vmr (dark crosses) and max vmr (dots) from REMS-H, and the min vmr
 529 from two column model annual simulations: 'reference' with I 300 and porosity 0.30 (regolith
 530 ground; solid line); 'rock' with I 400 and porosity 0.003 (exposed bedrock ground; dashed line).

531

532

533